Available online at www.sciencedirect.com
SCIENCE DIRECT®
Biochemical and Biophysical Research Communications 306 (2003) 169–176
BBRC
www.elsevier.com/locate/ybbrc

Existence of catalase-less peroxisomes in Sf21 insect cells☆

Mikinori Kurisu,[a,1] Masashi Morita,[a,1] Yoshinori Kashiwayama,[a] Sadaki Yokota,[b] Hiroshi Hayashi,[c] Yasuyoshi Sakai,[d] Shoji Ohkuma,[e] Mikio Nishimura,[c] and Tsuneo Imanaka[a,*]

[a] *Department of Biological Chemistry, Faculty of Pharmaceutical Sciences, Toyama Medical and Pharmaceutical University, 2630 Sugitani, Toyama 930-0194, Japan*
[b] *Biological Laboratory, Yamanashi University School of Medicine, 1100 Shimokatou, Tamaho 409-3898, Japan*
[c] *Department of Cell Biology, National Institute for Basic Biology, Okazaki 444-8585, Japan*
[d] *Division of Applied Life Sciences, Graduate School of Agriculture, Kyoto University, Sakyo-ku, Kyoto 606-8502, Japan*
[e] *Department of Biochemistry and Molecular Cell Biology, Faculty of Pharmaceutical Sciences, Kanazawa University, 13-1 Takara, Kanazawa 920-0934, Japan*

Received 25 April 2003

Abstract

Catalase activity, a peroxisomal marker enzyme, was not detectable in any of the subcellular fractions of *Spodoptera frugiperda* (Sf) 21 insect cells, although marker enzymes in other organelles were distributed in the fractions in a manner similar to that seen in mammalian cells. When a green fluorescent protein fused with peroxisome targeting signal 1 at the C-terminal (GFP-SKL) was expressed in Sf21 cells, punctate fluorescent dots were observed in the cytoplasm. The fraction where GFP-SKL was concentrated exhibited long-chain and very-long-chain fatty acid β-oxidation activities in the presence of KCN and the density of this fraction was slightly higher than that of mitochondria. Immunoelectron microscopy studies with anti-SKL antibody demonstrated that Sf21 cells have immunoreactive peroxisome-like organelles which are structurally distinct from mitochondria, endoplasmic reticulum, and lysosomes. In contrast to peroxisomal matrix proteins, adrenoleukodystrophy protein, a peroxisomal membrane protein, was not located to peroxisomes. This suggests that the targeting signal for PMP in insect cells is distinct from that in mammalian cells. These results demonstrate that Sf21 insect cells have unique catalase-less peroxisomes capable of β-oxidation of fatty acids.
© 2003 Elsevier Science (USA). All rights reserved.

Keywords: Peroxisome; Sf21 cells; Fatty acid β-oxidation; ABC protein; Peroxisome targeting signal; Adrenoleukodystrophy; Peroxisomal membrane protein

Peroxisomes are present in a wide variety of eukaryotic cells from yeast to human beings. They commonly contain oxidases that generate hydrogen peroxide and catalase that degrades the hydrogen peroxide. Fatty acid β-oxidation can proceed in both mitochondria and peroxisomes in mammalian cells whereas peroxisomes play an indispensable role in the oxidation of very-long-chain fatty acids ($>C_{22}$) and branched-chain fatty acids [1]. Peroxisomes also play an anabolic role in the biosynthesis of cholesterol, bile acids, and plasmalogen [2]. Peroxisomal matrix proteins are synthesized on free polysomes and transported to peroxisomes. Their targeting is controlled by the peroxisome targeting signal sequences, PTS1 and PTS2 [3]. In contrast, peroxisomal membrane proteins (PMPs) lack conserved signal sequences like PTS1 and PTS2, and their peroxisomal targeting system as yet is still unclear.

The baculovirus expression system has been used to express large quantities of a variety of functional eukaryotic recombinant proteins, including ATP-binding cassette (ABC) proteins such as *P*-glycoprotein [4], ABCG2 [5], and TAP [6]. With specific regard to the

☆ *Abbreviations:* ABC, ATP binding cassette; ALD, adrenoleukodystrophy; ALDP, adrenoleukodystrophy protein; AOx, acyl-CoA oxidase; GFP, green fluorescence protein; ML, mitochondrial and light mitochondrial; PMP, peroxisomal membrane protein; PTS, peroxisome targeting signal; Sf, *Spodoptera frugiperda*.

* Corresponding author. Fax: +81-76-434-4656.
E-mail address: imanaka@ms.toyama-mpu.ac.jp (T. Imanaka).

[1] Both authors contributed equally to this work.

0006-291X/03/$ - see front matter © 2003 Elsevier Science (USA). All rights reserved.
doi:10.1016/S0006-291X(03)00913-6

peroxisomal proteins, Chu et al. [7] have expressed large amounts of functionally active acyl-CoA oxidase (AOx), a rate-limiting enzyme for the β-oxidation of fatty acids in Sf9 insect cells. This overexpressed recombinant AOx, however, was distributed in both the cytoplasm and the nucleus in Sf9 cells. Alvares et al. [8] have reported that the insect cells exhibited no catalase-positive cytoplasmic organelles on immunofluorescence analysis. They have suggested the possibility that the distribution of the recombinant protein in cytoplasm was due to the absence of peroxisomes in the insect cells. We previously attempted to express recombinant peroxisomal ABC proteins in Sf21 cells to obtain large quantities of proteins for characterization. In baculovirus expression systems, abundant expression of adrenoleukodystrophy protein (ALDP), a peroxisomal ABC protein, has been achieved but the ALDP which was expressed was located on various membranes and exhibited crystalloid-like aggregates in nucleus. Thus, we had expected Sf21 cells would also not have any peroxisomes. To test this hypothesis, we attempted to express a green fluorescence protein fused with PTS1 at the C-terminal (GFP-SKL) in Sf21 cells using a vector transfection system since viral infection results in the production of a large quantity of recombinant proteins which eventually kill the insect cells. We had expected that the expressed GFP-SKL would be diffused in the cytoplasm. However, contrary to our expectation, GFP-SKL showed punctate fluorescent dots in the cytoplasm of Sf21 cells. Therefore, we investigated this distribution by subcellular fractionation followed by immunoblot analysis and immunoelectron microscopy using antibodies against GFP as well as SKL. In the present study, we provide evidence that Sf21 insect cells have previously unrecognized catalase-less peroxisomes.

Materials and methods

Materials. Rabbit anti-calreticulin, anti-SKL, and anti-GFP antibodies were purchased from StressGen Biotechnologies (Victoria, BC, Canada), Zymed Laboratories (South San Francisco, CA), and Clontech, respectively. Antipain, chymostatin, leupeptin, and pepstatin A were from the Peptide Institute (Osaka, Japan). ECL+Plus, a Western blotting detection system, and Fluorolink Cy3 labeled goat anti-rabbit IgG were obtained from Amersham Pharmacia Biotech. [1-^{14}C]Palmitoyl-CoA (60 mCi/mmol) and [1-^{14}C]lignoceric acid (53 mCi/mmol) were purchased from New Life Science Products (Boston, MA) and Moravek Biochemicals (California, USA), respectively. MitoTracker Red was from Molecular Probes (Leiden, The Netherlands). pIB/V5-His-TOPO vector, fetal calf serum (FCS), and Grace's Insect Medium were from Invitrogen. Rabbit anti-ALDP antibody raised against the COOH terminal 24 amino acids of human ALDP [9] was kindly provided by Dr. T. Yamada (Kyushu University, Japan).

Construction of pIB/GFP, GFP-SKL, and ALD. We have constructed three expression vectors, pIB/GFP, pIB/GFP-SKL, and pIB/ALD. The genes of interest were amplified with a PCR protocol using pEGFPN-1, pEGFP-SKL, and pcDNA3.1+/ALD as templates and cloned into a pIB/V5-His-TOPO vector by TA-cloning (Invitrogen). PCR was performed using two sets of oligonucleotide primers designed on the basis of their sequences: a forward primer (5′-ATCCACC GGTCGCCACCATG-3′) and a reverse primer (5′-CCTCTACAAA TGTGGTATGG-3′) for pIB/GFP and pIB/GFP-SKL, and a forward primer (5′-AGATATCCAGCACAGTGGCG-3′) and a reverse primer (5′-ATGGCTGGCAACTAGAAGGC-3′) for pIB/ALD. pEGFP-SKL was constructed as follows. PCR was performed with a forward primer (5′-CGCGGATCCATGGTGAGCAAGGGCGAGGAG-3′) having a *Bam*HI site and a reverse primer (5′-TAACTGCAGTTACA GCTTGCTCAGCTCGTCCATGCCGA-3′) having a *Not*I site using a pEGFPN-1 as template. The amplified PCR products were directly cloned into the *Bam*HI and *Not*I sites of pEGFPN-1 vector. cDNA sequences were confirmed by the dye-terminator cycle sequencing method using a DNA sequencer (ABI PRISM 310, PE Applied Biosystems).

Expression of GFP, GFP-SKL, and ALDP in Sf21 insect cells. The insect host culture of Sf21 cells was obtained from Invitrogen. Cell cultures were grown in a modified Grace's insect cell culture medium containing 10% FCS and 10 μg/ml gentamicin. Sf21 cells were seeded on six-well tissue culture dishes at about 1×10^5 cells/well. After 30 min at 27 °C, they were transfected with the vector plasmid (pIB/GFP, pIB/GFP-SKL, and pIB/ALD) using calcium phosphate methods, following the manufacturer's instructions. Two micrograms of plasmid was used for each transfection. After 3 days incubation, the cells were subcultured in a (the) medium containing 50 μg/ml Blasticidin S hydrochloride.

Subcellular fractionation of Sf21 cells. Fractionation was carried out as described previously [10]. Ninety percent confluent cells in 75-cm^2 culture flasks were washed three times with phosphate-buffered saline (PBS). The cells were homogenized with a Teflon/glass Potter–Elvehjem homogenizer in 10 volumes of homogenization buffer (0.25 M sucrose, 1 mM EDTA, and 0.1% (w/v) ethanol, pH 7.0, containing 3 mM imidazole) at 4 °C. The homogenate was first fractionated by different centrifugations to prepare the mitochondrial and light mitochondrial (ML) fractions according to the method of de Duve et al. [11]. The ML fraction was further subjected to equilibrium density centrifugation in a 10.6-ml linear sucrose gradient (1.10–1.17 g/ml) in a Beckman NVT65 rotor. The gradient rested on 0.5 ml of 1.27 g/ml sucrose. The centrifugation was carried out at 193,000*g* for 90 min at 4 °C. The gradient was collected in preweighted microtubes as approximate 1.0 ml fractions from the bottom of the tube, and the density of each fraction was determined by refractometry. Leupeptin, antipain, chymostatin, and pepstatin A were added, each maintained at the final concentration of 10 μg/ml throughout the process.

Immunofluorescence and immunoelectron microscopy. Immunofluorescence microscopy was performed as described previously [12] with certain modifications. Sf21 cells were permeabilized by 100% methanol for 20 min at room temperature. After blocking with 3% (w/v) bovine serum albumin (BSA) in PBS for 1 h, cells were incubated with anti-calreticulin antibody followed with Cy3-conjugated anti-rabbit IgG. The cells were mounted in 90% glycerol in 100 mM Tris–HCl (pH 8.0) and the samples were examined by confocal microscopy (Carl Zeiss LSM510, Jena, Germany). We also used MitoTracker Red according to the manufacturer's instructions to detect mitochondria. Immunoelectron microscopy of Sf21 cells with anti-SKL or anti-GFP antibody was performed as described previously [13].

β-Oxidation activity assay. Palmitoyl-CoA and lignoceroyl-CoA oxidation activities were measured according to Lazarow [14] with certain modifications. The oxidation reaction was carried out with 500 μl of 50 mM Tris–HCl buffer (pH 8.0) containing 10 μM unlabeled palmitoyl- or lignoceroyl-CoA, 0.1 mM coenzyme A, 0.2 mM NAD^+, 1 mM dithiothreitol, 0.75% (v/v) BSA, 0.01 mM FAD, 0.01% (w/v) of Triton X-100, and 1 nmol [1-^{14}C]palmitoyl- or lignoceroyl-CoA. In some experiments, 1 mM KCN was added to the reaction. The reaction was started by the addition of peroxisomal fractions. After incubation for 10 min at 37 °C, reactions were terminated by adding 250 μl of ice-cold 3 M perchloric acid to the reaction mixture, and the

mixture was incubated for 1 h on ice. After centrifugation, the supernatant was extracted twice with 1.5 ml of hexane. The acid-soluble radioactivities in the aqueous phase were measured by a scintillation counter.

Other methods. [1-^{14}C]Lignoceroyl-CoA was synthesized as described previously by Yamashita et al. [15]. Enzyme activities of catalase, *N*-acetyl-β-D-glucosaminidase, cytochrome *c* oxidase, and NADPH cytochrome *c* reductase were assayed as described previously [10]. Immunoblotting was done by the method of Small et al. [12] using ECL+Plus, a Western blotting detection system. Protein concentration was measured by the method of Bradford [16] with a protein assay kit (Bio-Rad) using bovine plasma γ-globulin as the standard.

Results

Subcellular fractionation of Sf21 cells and no catalase activity in the cells

Organelles from Sf21 cells were separated by a sucrose density gradient centrifugation and marker enzymes were measured. As shown in Fig. 1, the enzyme activities against mitochondria, lysosomes, and endoplasmic reticulum (ER) were well separated and their distributions were similar to those of mammalian cells such as rat hepatoma H-4-II-E cells [10] and CHO cells [12]. In mammalian cells, the density of peroxisomal fraction where the catalase is recovered is always higher than that of mitochondrial fraction where cytochrome *c* oxidase is recovered. In Sf21 cells, however, catalase activity was not detected in any fractions. In our catalase assay, decrease of hydrogen peroxide in the incubation was determined colorimetrically using titanium (IV) oxysulfate. However, more than 1 mg of protein from homogenate, nuclear, postnuclear supernatant, ML, and soluble fractions did not make the absorbance decrease.

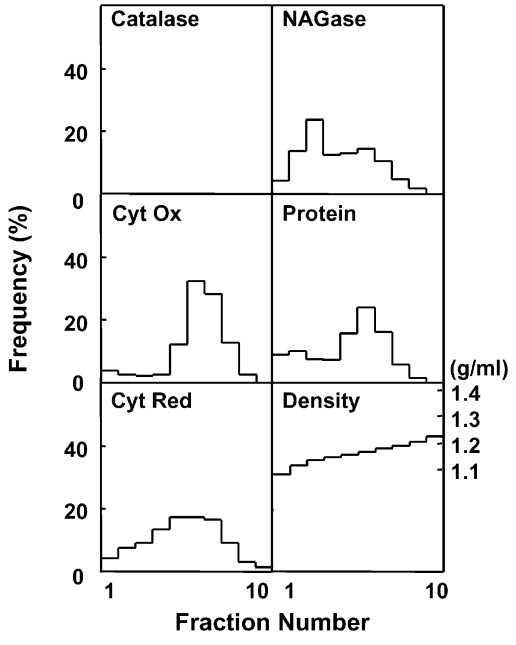

Fig. 1. Subcellular fractionation of Sf21 insect cells. Mitochondrial and light mitochondrial (ML) fractions prepared from Sf21 cells were fractionated by an equilibrium density centrifugation on sucrose. The marker enzyme distributions are plotted; cytochrome *c* oxidase (Cyt Ox), NADPH cytochrome *c* reductase (Cyt Red), and *N*-acetyl-β-D-glucosaminidase (NAGase) were measured as marker enzymes of mitochondria, microsomes, and lysosomes, respectively. The recovery of each constituent in the gradient ranged from 80% to 110%. Catalase activity was not detected in Sf21 cells.

PTS directs a green fluorescent protein to peroxisome-like structure in Sf21 cells

It has been well characterized that a tripeptide PTS (Ser–Lys–Leu) located at the C terminus of a majority of peroxisomal matrix proteins targets the proteins to peroxisomes [17]. To define the existence of peroxisome-like organelle in Sf21 cells, we first attempted to express GFP fused with SKL at C-terminal (GFP-SKL). Viral infection kills the insect cells, making it difficult to observe post-translational protein sorting in living cells, so that we have used a vector transfection system to express GFP-SKL. The Sf21 cells were transfected with pIB/GFP-SKL or pIB/GFP and the stable transformants were cloned by a Blasticidin S selection. The cells stably expressing GFP-SKL (Fig. 2A, right panel) showed punctate fluorescent dots that were found in the particulate fraction of the cells. When GFP lacking PTS1 was expressed in the cells, a diffuse fluorescence pattern was observed in the cytoplasm (Fig. 2A, left panel). These results suggest that SKL functions as PTS1 in Sf21 cells. To identify the subcellular distribution of the expressed GFP-SKL, Sf21 cells stably expressing GFP-SKL were fractionated as in Fig. 1 and each fraction was subjected to immunoblot analysis with anti-GFP antibody (Fig. 2B). A predominant immunoreactive protein having a molecular weight of 30 kDa appeared to be distributed mainly at fractions 8 and 9, and the peak fraction was denser than those of the marker enzymes of mitochondria. These results clearly demonstrate that GFP-SKL targets to restricted organelle distinguished from mitochondria, lysosomes, and ER.

Fatty acid β-oxidation activities in Sf21 cells

In primary experiments, we have found that Sf21 cells oxidized lignoceric acid to water-soluble products. The activity of lignoceric acid β-oxidation was ~40 pmol/mg/h in Sf21 cells and the activity was ~1/10 of human fibroblasts. To determine whether the punctuate dots of GFP-SKL resulted in targeting to peroxisomes where fatty acid β-oxidation activity exists, we measured the capacity of fatty acid β-oxidation in the gradient fractions. Density gradient centrifugation of the ML fraction showed that the KCN-sensitive β-oxidation activity

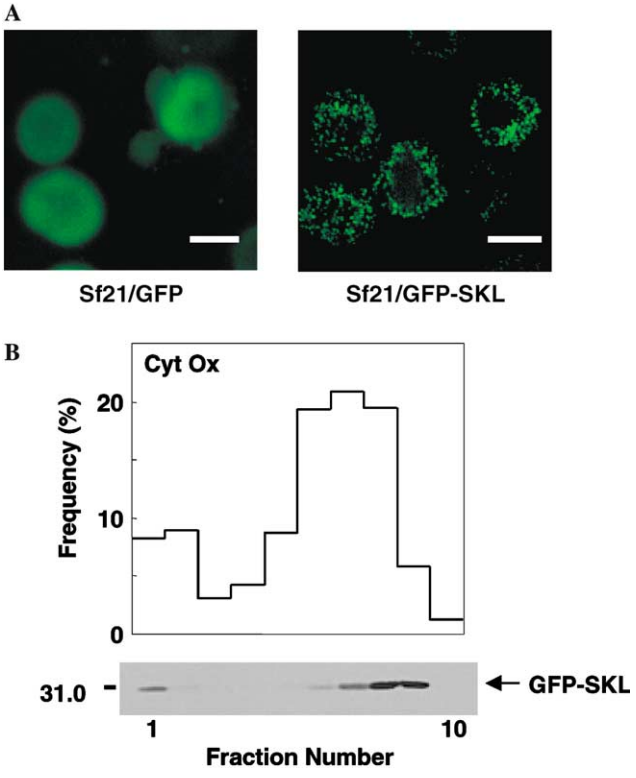

Fig. 2. Expression of GFP-SKL in Sf21 insect cells. GFP-SKL or GFP was stably expressed in Sf21 cells. The localization of GFP-SKL was analyzed by immunofluorescence and subcellular fractionations followed by immunoblotting. (A) Fluorescence of GFP (left) or GFP-SKL (right) in Sf21 cells was observed with a confocal laser scan microscopy (Bar = 10 μm). (B) ML fraction from Sf21 cells stably expressing GFP-SKL was fractionated by a sucrose gradient centrifugation as in Fig. 1. Cytochrome *c* oxidase (Cyt Ox) activity was measured as a marker enzyme of mitochondria. Immunoblot analysis of each fraction was done using anti-GFP antibody.

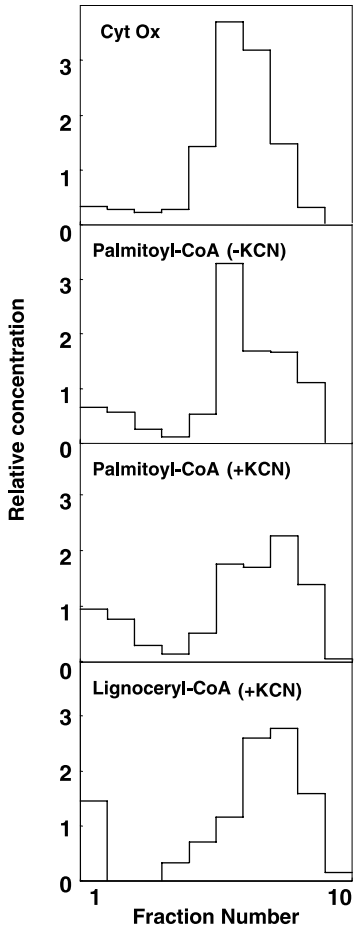

Fig. 3. β-Oxidation activity of [1-^{14}C]palmitoyl-CoA and [1-^{14}C]lignoceroyl-CoA in fractions prepared from Sf21 insect cells. Subcellular fractionation of Sf21 cells was done as in Fig. 1. β-Oxidation activity of the each fraction was measured using [1-^{14}C]palmitoyl-CoA or [1-^{14}C]lignoceroyl-CoA as substrates. Aliquots of the each fraction were incubated with [1-^{14}C]palmitoyl-CoA or [1-^{14}C]lignoceroyl-CoA in the absence or presence of KCN for 10 min at 37 °C. Cytochrome *c* oxidase (Cyt Ox) activity was measured as a marker enzyme of mitochondria. The recoveries of the enzyme activity in the gradient ranged from 80% to 130%.

was mainly detected in the fraction corresponding to mitochondria (fraction 6) (Fig. 3) when [1-^{14}C]palmitic acid was used as substrate. In contrasts, KCN-insensitive activity was distributed in fraction 8. When lignoceric acid, a very-long-chain fatty acid, was used as substrate, the activity was associated mainly in fractions 7 and 8 where GFP-SKL was located. Long-chain fatty acid can be oxidized by both mitochondria and peroxisomes, and the mitochondrial β-oxidation is known to be inhibited in the presence of KCN. Very-long-chain fatty acid ($>C_{22}$) oxidation occurs exclusively in the peroxisomal matrix and can therefore serve as a marker for peroxisome function. These studies clearly indicate that the organelles where GFP-SKL was located were peroxisomes capable of β-oxidizing fatty acids.

Identification of peroxisomes by immunofluorescence and immunoelectron microscopy

Sf21 cells expressing GFP-SKL had punctate fluorescent dots and the staining pattern was distinguished from those of calreticulin, an ER luminal resident protein (Fig. 4, upper). The fluorescent dots derived from mitotracker did not superimpose to those of GFP-SKL (Fig. 4, lower) although some of the fluorescence derived from mitotracker was overlapped with those of GFP-SKL. To further determine the cellular localization of GFP-SKL, immunoelectron microscopy study with anti-GFP antibodies was performed. As shown in Fig. 5A, the gold particles were associated with one or two small, spherical structures which were distinguishable from endosomes, lysosomes, and mitochondria. This is consistent with descriptions of peroxisomes found by electron microscopy of serial sections of rat liver and yeast [18]. Further, we attempted to identify peroxisomes in Sf21 cells by an anti-SKL antibody as a probe for endogenous peroxisomal matrix protein. As shown in Fig. 5B, the gold particles were found over organelles that

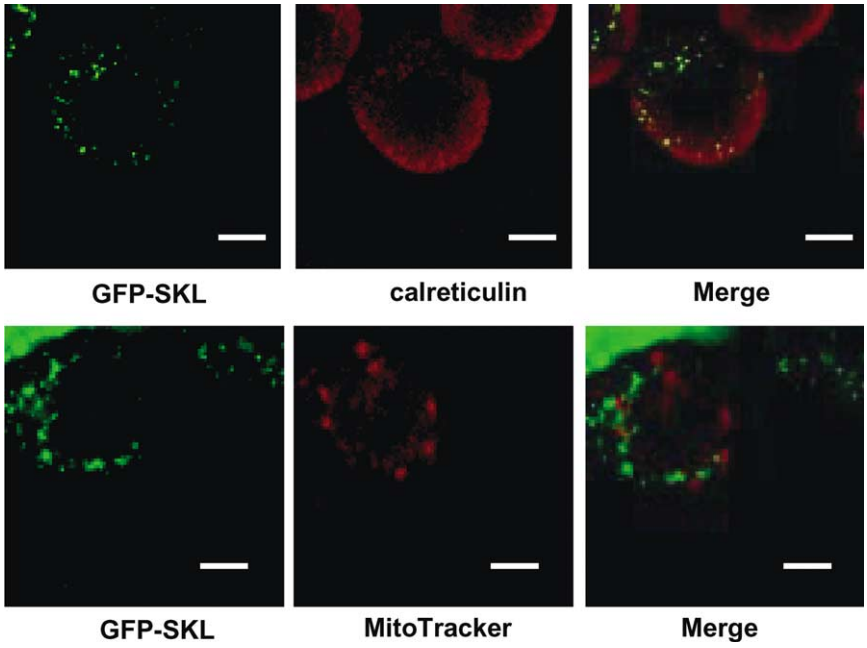

Fig. 4. Localization of GFP-SKL expressed in Sf21 cells. Sf21 cells stably expressing GFP-SKL were fixed with 10% (w/v) paraformaldehyde and permeabilized with 100% methanol. After blocking with 3% (w/v) BSA in PBS for 1 h, cells were incubated for 1 h with anti-calreticulin antibody. Cells were then incubated for 1 h with Cy3-conjugated anti-rabbit IgG. MitoTracker Red was also used for detecting mitochondria. Fluorescence was observed with a confocal microscopy. The fluorescence dots of the MitoTracker (mitochondria) and calreticulin (endoplasmic reticulum) were not superimposed to that of GFP-SKL though some of the GFP-SKL appeared to be localized in mitochondria. Bar = 5 μm.

were structurally identical to those shown in Fig. 5A. On the basis of these data, we concluded that Sf21 cells have typical peroxisomes lacking catalase.

ALDP was not localized to peroxisomes

To characterize the localization of ALDP, a PMP, we attempted to express ALDP in Sf21 cells using a vector transfection system. Unexpectedly, however, ALDP was distributed predominantly in plasma membrane, endosomes, lysosome-like structures or nucleus as visualized at the electron microscopic level (Fig. 6A). We did not observe concentrated protein A-gold dots in peroxisomes as in Fig. 5. Subcellular fractionation followed by immunoblot analysis also showed that ALDP was distributed in various fractions, especially in mitochondria (Fig. 6B). This mislocalization of ALDP indicates that PTS of ALDP did not function in insect cells.

Discussion

Recent studies have demonstrated that baculovirus-expressed AOx and urate oxidase are distributed in the cytoplasm and nucleus, and did not locate to a specific organelle in Sf9 cells [7,8,18]. We also observed that ALDP expressed by a baculovirus-mediated expression system was localized to various membranes and exhibited crystalloid-like aggregates in the nucleus in Sf9 and Sf21 cells (data not shown). Based on these lines of evidence, we had thought that Sf21 cells did not possess any peroxisomes. Thus, we had expected that GFP-SKL would be diffused in the cytoplasm, when we attempted to express GFP-SKL using a vector-transfection system. However, GFP-SKL exhibited as punctate fluorescent dots in the cytoplasm (Fig. 2A). The existence of peroxisomes in Sf21 is supported by the following findings. (1) The organelle containing GFP-SKL was recovered in a fraction denser than the mitochondrial fraction by means of sucrose gradient centrifugation (Fig. 2B). (2) This organelle was capable of oxidizing both long- and very-long-chain fatty acids and these activities were not inhibitable with KCN, a known inhibitor of the mitochondrial oxidation pathway (Fig. 3), indicating that this organelle is not a mitochondrion. This is also supported by the report that the β-oxidation of very-long-chain fatty acids more than 22 carbons in length is limited to peroxisomes. (3) The immunofluorescence pattern of GFP-SKL was not superimposable on the distribution of calreticulin and MitoTracker (Fig. 4). (4) On immunoelectron microscopy study, immunogold particles exhibiting GFP-SKL appeared to be concentrated at restricted organelles structurally different from the nuclei, mitochondria or lysosomes. (5) When an anti-SKL antibody was used as a probe for endogenous peroxisomal matrix proteins in Sf21 cells, the immunogold particles appeared to be located in organelles that were structurally identical to those observed in the case

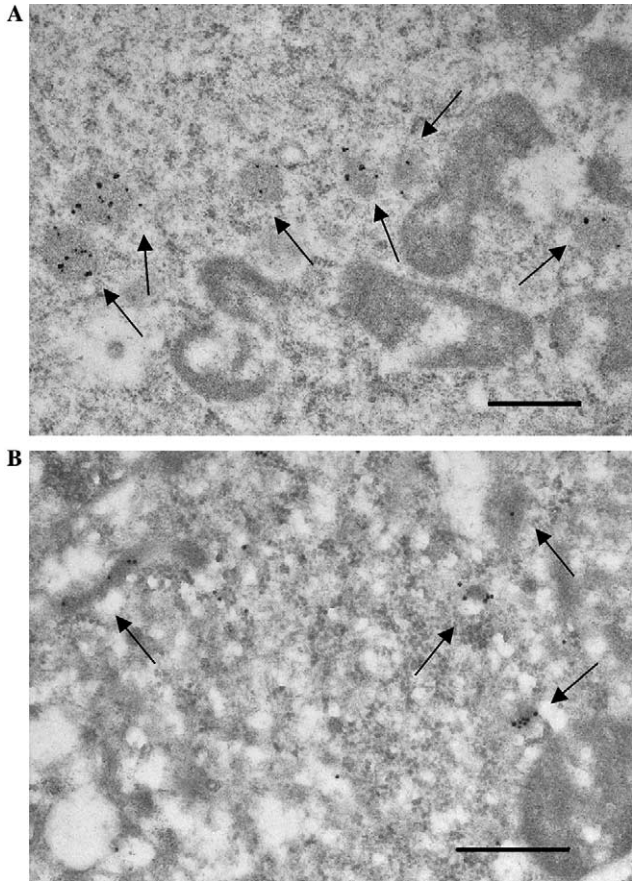

Fig. 5. Immunoelectron microscopy of Sf21 and Sf21/GFP-SKL cells. (A) Immunogold staining of Sf21 cells stably expressing GFP-SKL was done using anti-GFP antibody. Gold particles exhibiting GFP-SKL were restricted to organelles that were distinguishable from mitochondria or nucleus. Bar = 0.5 μm. (B) Endogenous peroxisomal proteins with SKL residues at C-terminal were detected using anti-SKL antibody. Immunogold particles appeared to be in structurally similar organelles as in A (shown by arrows). Bar = 0.5 μm.

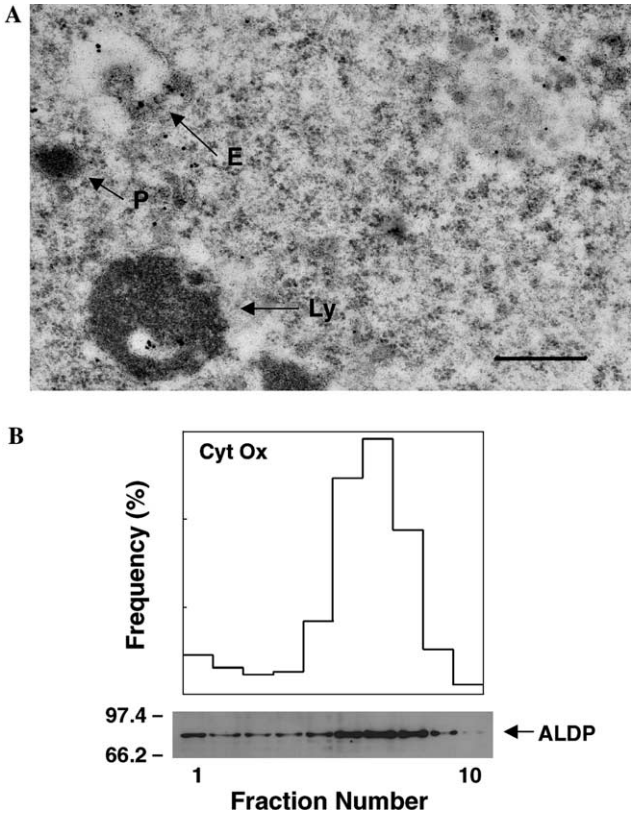

Fig. 6. Localization of ALDP expressed in Sf21 insect cells. (A) Immunoelectron micrographs of Sf21 cells expressing ALDP. Immunostaining was done using an anti-ALDP antibody. Gold particles exhibiting ALDP were observed in both endosomes and lysosomes as indicated by arrows. P, peroxisome; E, endosome; and Ly, lysosome. Bar = 0.5 μm. (B) Subcellular fractionation of Sf21 cells followed by immunoblot analysis of ALDP. Sf21 cells were fractionated as in Fig. 1. Cytochrome *c* oxidase (Cyt Ox) was measured as a marker enzyme of mitochondria. The recovery of the activity in the gradient was 92%. An aliquot of each fraction from the top (fraction 1) to the bottom (fraction 10) was removed and subjected to SDS–PAGE followed by immunoblotting. ALDP appeared to be distributed in all fractions, especially in mitochondria.

of the GFP-SKL containing cells (Fig. 5A). Therefore, the mislocalization of the peroxisomal matrix proteins such as AOx and urate oxidase in the earlier studies is not due to the absence of peroxisomes, but rather, due to the small number of peroxisomes present. The number of peroxisomes appears to be too low to accept the large amounts of heterologous proteins produced by the baculovirus-mediated expression systems.

One of the interesting points in this study is that catalase activity was not detected in Sf21 by means of enzymatic assay. The catalase molecule was also not detected by immunoblot analysis of anti-catalase antibodies against several species. We also did not detect catalase molecules or catalase activity in Sf9 cells either (data not shown). These findings are consistent with the previous observation that Sf9 cells showed no catalase-positive cytoplasmic organelles upon immunofluorescence analysis [8]. Various kinds of oxidative metabolism occur as a result of hydrogen peroxide-generating oxidase in peroxisomes. As hydrogen peroxide is cytotoxic and can cause very serious damage to cellular components, it must be decomposed. It has been reported that hydrogen peroxide is scavenged not only by catalase but also by glutathione peroxidase in cells ranging from yeast to mammalian cells [19]. In yeast *Candida boidinii*, CbPmp20 utilizes glutathione peroxidase activity as well as catalase in eliminating hydrogen peroxide [20]. Thus, certain kinds of peroxidases to decompose hydrogen peroxide could well exist in Sf21 cells in a like manner, although we have not been able to detect glutathione peroxidase activity to date.

Another interesting point which arose in this study is that heterologous peroxisomal membrane proteins (PMPs) did not locate to peroxisomes, although peroxisomal matrix proteins were targeted to the peroxisome via a PTS1 targeting system. In the present study, we

have attempted to express ALDP using a vector transfection system. Unexpectedly, however, the expression of ALDP in peroxisomal membranes failed. We were able to express other PMPs in Sf21 cells, such as PMP70 and ALDP-related protein, but these PMPs were also mislocated to other membranes (data not shown). In X-ALD fibroblasts, overexpressed ALDP was correctly located in peroxisomes and restored the β-oxidation activity of very-long-chain fatty acids [21]. As expected, expression of ALDP in Sf21 cells did not show any increases in activity, suggesting that ALDP was not transported to peroxisomes. One possible explanation is that peroxisomal membranes have a limited capacity to accept ALDP. However, it is unlikely that there were any PMPs which were not transported to peroxisomes since the amount of expressed ALDP was less than that of GFP-SKL. Another possibility is that the targeting system of PMPs in insect cells may be different from that in mammalian cells. It has been reported that Pex19p, Pex3p, and Pex16p have a role in targeting, integration, and orientation of PMPs in yeast and mammalian cells [22]. A conserved signal sequence in PMPs for targeting, however, has not yet been identified. In contrast to peroxisomal matrix proteins, systems targeting PMPs might be diverse in insect cells. As ALDP has been shown to be required for the β-oxidation of very-long-chain fatty acids in peroxisomes [21,23], it is of great interest to know what kinds of PMPs have a role in the fatty acid β-oxidation and how the PMPs are targeted to peroxisomes in insect cells.

In early studies insect peroxisomes were first described from the fifth stage of *Calpodes* fat bodies where they contain both catalase and urate oxidase [24]. It has been reported that peroxisomes undergo a repeating cycle of formation and destruction during insect development. For example, peroxisomes are formed at the beginning of the fourth stadium and are lost after ecdysis to the fifth. They are formed again at the beginning of the fifth stadium and are lost once again prior to pupation. They form once again at the end of the pupal stage during formation of the adult stage [25]. Peroxisomes are thus thought to be an organelle that is formed only for use in a particular stadium as it undergoes repeating cycles of formation and loss. The insect cell lines, Sf9 and Sf21, were originally established from the ovarian tissues of *Spodoptera frugiperda* larvae. Therefore, Sf21 and Sf9 cells would appear to be an interesting and highly useful tool to help understand both the biogenesis and diversity of peroxisomes. In addition, in rodents, the number of peroxisomes is highly inducible by treatment with peroxisome proliferators such as fenofibrate or free fatty acids [26–28] that activate PPARs. In yeast cells, although only a few small peroxisomes are detectable under normal growth conditions, their number may be induced by a medium containing oleic acid [29]. If some compounds are able to induce peroxisomes in Sf21 cells, the cells might provide useful information towards an understanding of the diversity of peroxisomes.

In the present study, we have demonstrated the existence of catalase-less peroxisomes in Sf21 cells. We have also shown that the mechanism for matrix protein import into peroxisomes is highly conserved during the evolutionary process, but for PMPs, which might have a greater than usual degree of diversity. The targeting mechanism of the PMPs as well as the induction of peroxisomes in Sf21 cells are both now under active investigation.

Acknowledgments

We thank Dr. Yamada (Kyushu University) and Dr. Kamijo (Shinshu University) for providing us anti-ALDP antibody and pcDNA3.1+/ALD, respectively. We thank Dr. Kevin Boru of Advanced Clinical Trials for review of the manuscript. This work was supported in part by a Grant-in-Aid for Scientific Research from the Ministry of Education, Culture, Sports, Science and Technology of Japan (10217205 and 14370740) and grants from The Hokuriku Industrial Advancement Center and The Fugaku Trust for Medicinal Research.

References

[1] J.K. Reddy, G.P. Mannaerts, Peroxisomal lipid metabolism, Annu. Rev. Nutr. 14 (1994) 343–370.
[2] H. van den Bosch, R.B.H. Schtgens, R.J.A. Wanders, J.M. Tager, Biochemistry of peroxisomes, Annu. Rev. Biochem. 61 (1992) 157–197.
[3] S. Subramani, Protein import into peroxisomes and biogenesis of the organelle, Annu. Rev. Cell. Biol. 9 (1993) 445–478.
[4] U.A. Germann, Baculovirus-mediated expression of human multidrug resistance cDNA in insect cells and functional analysis of recombinant P-glycoprotein, Methods Enzymol. 292 (1998) 427–441.
[5] C. Özvegy, T. Litman, G. Szakács, Z. Nagy, S. Bates, A. Váradi, B. Sarkadi, Functional characterization of the human multidrug transporter, ABCG2, expressed in insect cells, Biochem. Biophys. Res. Commun. 285 (2001) 111–117.
[6] S. Uebel, T. Plantinga, P.J.A. Weber, A.G. Beck-Sickinge, R. Tampé, Peptide binding and photo-crosslinking to detergent solubilized and to reconstituted transporter associated with antigen processing (TAP), FEBS Lett. 416 (1997) 359–363.
[7] R. Chu, N. Usuda, M.K. Reddy, C. Liu, T. Hashimoto, K. Alvares, M.S. Rao, J.K. Reddy, Functional expression of rat peroxisomal acyl-CoA oxidase in *Spodoptera frugiperda* cells, Biochem. Biophys. Res. Commun. 200 (1994) 178–186.
[8] K. Alvares, R.J. Widrow, G.M. Abu-Jawdeh, J.V. Schmidt, A.V. Yeldandi, M.S. Rao, J.K. Reddy, Rat urate oxidase produced by recombinant baculovirus expression: formation of peroxisome crystalloid core-like structures, Proc. Natl. Acad. Sci. USA 89 (1992) 4908–4912.
[9] T. Kobayashi, T. Yamada, T. Yasutake, N. Shinnoh, I. Goto, T. Iwaki, Adrenoleukodystrophy gene encodes an 80 kDa membrane protein, Biochem. Biophys. Res. Commun. 201 (1994) 1029–1034.
[10] T. Imanaka, Y. Shiina, T. Takano, T. Hashimoto, T. Osumi, Insertion of the 70-kDa peroxisomal membrane protein into

peroxisomal membranes in vivo and in vitro, J. Biol. Chem. 271 (1996) 3706–3713.
[11] C. de Duve, B.C. Pressman, R. Gianetto, R. Wattiaux, F. Appelmans, Tissue fractionation studies. 6. Intracellular distribution patterns of enzymes in rat liver tissue, Biochem. J. 60 (1955) 604–617.
[12] T. Imanaka, K. Aihara, T. Takano, A. Yamashita, R. Sato, Y. Suzuki, S. Yokota, T. Osumi, Characterization of the 70-kDa peroxisomal membrane protein, an ATP binding cassette transporter, J. Biol. Chem. 274 (1999) 11968–11976.
[13] S. Yokota, K. Kamijo, T. Oda, Aggregate formation and degradation of overexpressed wild-type and mutant urate oxidase proteins. Quality control of organelle-destined proteins by the endoplasmic reticulum, Histochem. Cell Biol. 114 (2000) 433–446.
[14] P.B. Lazarow, Assay of peroxisomal β-oxidation of fatty acids, Methods Enzymol. 72 (1981) 315–319.
[15] A. Yamashita, M. Watanabe, T. Tonegawa, T. Sugiura, K. Waku, Acyl-CoA binding and acylation of UDP-glucuronosyltransferase isoforms of rat liver: their effect on enzyme activity, Biochem. J. 312 (1995) 301–308.
[16] M.M. Bradford, A rapid and sensitive method for the quantitation of microgram quantities of protein utilizing the principle of protein–dye binding, Anal. Biochem. 72 (1976) 248–254.
[17] S. Miura, I. Kasuya-Arai, H. Mori, S. Miyazawa, T. Osumi, T. Hashimoto, Y. Fujuki, Carboxyl-terminal consensus Ser-Lys-Leu-related tripeptide of peroxisomal proteins functions in vitro as a minimal peroxisome-targeting signal, J. Biol. Chem. 267 (1992) 14405–14411.
[18] R. Chu, U. Varanasi, S. Chu, Y. Lin, N. Usuda, M.S. Rao, J.K. Reddy, Overexpression and characterization of the human peroxisomal acyl-CoA oxidase in insect cells, J. Biol. Chem. 270 (1995) 4908–4915.
[19] T.B. Dansen, K.W. Wirtz, The peroxisome in oxidative stress, IUBMB Life 5 (2001) 223–230.
[20] H. Horiguchi, H. Yurimoto, N. Kato, Y. Sakai, Antioxidant system within yeast peroxisome. Biochemical and physiological characterization of CbPmp20 in the methylotrophic yeast *Candida Boidinii*, J. Biol. Chem. 276 (2001) 14279–14288.
[21] G. Unterrainer, B. Molzer, S. Forss-Petter, J. Berger, Co-expression of mutated and normal adrenoleukodystrophy protein reduces protein function: implications for gene therapy of X-linked adrenoleukodystrophy, Hum. Mol. Gen. 9 (2000) 2609–2616.
[22] P.E. Purdue, P.B. Lazarow, Peroxisome biogenesis, Annu. Rev. Cell Dev. Biol. 17 (2001) 701–752.
[23] J. Mosser, A.M. Douar, C.-O. Sarde, P. Kioschis, R. Feuil, H. Moser, A.-M. Poustka, J.-L. Mandel, P. Aubourg, Putative X-linked adrenoleukodystrophy gene shares unexpected homology with ABC transporters, Nature 361 (1993) 726–730.
[24] M. Locke, J.T. McMahon, The origin and fate of microbodies in the fat body of an insect, J. Cell Biol. 48 (1971) 61–78.
[25] W.J. Larsen, Cell remodeling in the fat body of an insect, Tissue Cell 8 (1976) 73–92.
[26] R. Hess, R. Stäubli, W. Reiss, Nature of the hepatomegalic effect produced by ethyl-chlorophenoxy-isobutyrate in the rat, Nature 208 (1965) 856–858.
[27] D.J. Svoboda, O.L. Azarnoff, Response of hepatic microbodies to a hypolipidemic agent, ethyl-chlorophenoxyisobutyrate (CPIB), J. Cell Biol. 30 (1969) 442–450.
[28] J.K. Reddy, T.P. Krishnakantha, Hepatic peroxisome proliferation: induction by two novel compounds structurally unrelated to clofibrate, Science 190 (1975) 787–789.
[29] M. Veenhuis, M. Mateblowski, W.H. Kunau, W. Harder, Proliferation of microbodies in *Saccharomyces cerevisiae*, Yeast 3 (1987) 77–84.